

Contents lists available at ScienceDirect

Bioactive Materials

journal homepage: www.keaipublishing.com/en/journals/bioactive-materials





Dual-sized hollow particle incorporated fibroin thermal insulating coatings on catheter for cerebral therapeutic hypothermia

Ming Li ^{a,1}, Yuan Gao ^{b,1}, Miaowen Jiang ^{c,1}, Hongkang Zhang ^d, Yang Zhang ^a, Yan Wu ^a, Wenhao Zhou ^e, Di Wu ^a, Chuanjie Wu ^a, Longfei Wu ^a, Luzi Bao ^a, Xiaoxiao Ge ^c, Zhengfei Qi ^c, Ming Wei ^c, Ang Li ^f, Yuchuan Ding ^g, Jicheng Zhang ^h, Guangzhen Pan ^h, Yu Wu ^h, Yan Cheng ^d, Yufeng Zheng ^{d,*}, Xunming Ji ^{a,b,c,i,**}

- a China-America Institute of Neuroscience and Beijing Institute of Geriatrics, Xuanwu Hospital, Capital Medical University, Beijing, 100053, China
- ^b School of Instrumentation and Optoelectronic Engineering, Beihang University, Beijing, 100191, China
- Beijing Institute for Brain Disorders, Capital Medical University, Beijing, 100069, China
- ^d School of Materials Science and Engineering, Peking University, Beijing, 100871, China
- ^e Shaanxi Key Laboratory of Biomedical Metallic Materials, Northwest Institute for Nonferrous Metal Research, Xi'an, 710016, China
- f Department of Biomedical Engineering, Columbia University, New York City, NY, 10027, USA
- g Department of Neurosurgery, Wayne State University School of Medicine, Detroit, MI, 48201, USA
- h Gong Yi Van-research Innovation Composite Material Co. Ltd, Zheng Zhou, 451299, China
- ¹ Department of Neurosurgery, Xuanwu Hospital, Capital Medical University, Beijing, 100053, China

ARTICLE INFO

Keywords: Silk fibroin Thermal insulation coating Catheter Stroke Hypothermia

ABSTRACT

Selective endovascular hypothermia has been used to provide cooling-induced cerebral neuroprotection, but current catheters do not support thermally-insulated transfer of cold infusate, which results in an increased exit temperature, causes hemodilution, and limits its cooling efficiency. Herein, air-sprayed fibroin/silica-based coatings combined with chemical vapor deposited parylene-C capping film was prepared on catheter. This coating features in dual-sized-hollow-microparticle incorporated structures with low thermal conductivity. The infusate exit temperature is tunable by adjusting the coating thickness and infusion rate. No peeling or cracking was observed on the coatings under bending and rotational scenarios in the vascular models. Its efficiency was verified in a swine model, and the outlet temperature of coated catheter (75 µm thickness) was 1.8–2.0 °C lower than that of the uncoated one. This pioneering work on catheter thermal insulation coatings may facilitate the clinical translation of selective endovascular hypothermia for neuroprotection in patients with acute ischemic stroke.

1. Introduction

Acute ischemic stroke (AIS) is the major cause of mortality and disability [1], with a global incidence of around 101.3 per 100,000 population [2]. Intravenous thrombolysis or mechanical thrombectomy, due to the lack of effective neuroprotective measures, is only effective in ideal scenarios, and thus still facing the challenge of poor prognosis [3, 4]. Unfortunately, almost all of the pharmaceutical approaches for

neuroprotection that effective in preclinical setting turned out to be ineffective in large clinical trials [5]. Therapeutic hypothermia is a promising adjuvant treatment for AIS with improved outcomes [6].

Intra-arterial selective cooling infusion (IA-SCI) displayed faster cooling rate and minimized side effects that existed in systemic therapeutic hypothermia (such as shivering and pneumonia) [7–9], especially compared with traditional endovascular cooling and surface cooling. IA-SCI mainly utilized an endovascular catheter to achieve the infusion

Peer review under responsibility of KeAi Communications Co., Ltd.

E-mail addresses: yfzheng@pku.edu.cn (Y. Zheng), jixm@ccmu.edu.cn (X. Ji).

^{*} Corresponding author.

^{**} Corresponding author. China-America Institute of Neuroscience and Beijing Institute of Geriatrics, Xuanwu Hospital, Capital Medical University, Beijing, 100053, China.

¹ These authors contributed equally to this paper.

of cooling fluid (e.g. ice-cold saline, human albumin, Ringer lactate solution or autologous blood) into the ischemic territory from the femoral artery to carotid artery as illustrated in Fig. 1a. However, the standard catheter used in IA-SCI is not inherently designed for cerebral hypothermia therapy, and displays a comparable coefficient of thermal conductivity (0.341 W m⁻¹ K⁻¹) [10] to that of blood (0.5 W m⁻¹ K⁻¹) [11]. This shortcoming inevitably causes the warming of the cold perfusate within the catheter as shown in Fig. 1b [12] and reduces the potency of the hypothermia treatment for AIS [13]. For example, an in vitro phantom experiment indicated that the temperature of the 33 mL/min cold saline within the 5F interventional catheter increased from 5.4 \pm 0.41 °C (at the initial femoral inflow site) to 25.21 \pm 0.49 °C (at the distal tip of catheter in carotid artery) [14]. Current studies focus on making catheters with novel designs to improve their cooling performance by minimizing the heat exchange of the cold infusion fluid within catheter with the outside warm blood and tissues, such as balloon-wrapping [15], balloon-coaxial (TwinFlo@) [16] and coaxial configurations [13]. However, these cooling catheters are complicated to be manufactured and expensive, lack flexibility, and cannot be inserted into some target vessels due to their increased diameters. Therefore, novel and facile approaches should be provided to endow the catheter wall with increased thermal resistant properties.

Developing the biocompatible thermal resistant coatings on catheters by surface engineering technique is an effective strategy to ameliorate the warming effects on infusate. Traditional thermal insulation coatings are mainly made of non-cyto/hemocompatible ceramics, polymers or composites, and commonly used in the industrial application (e.g. building construction, space technology, and power generation) [17–19]. However, these coatings are thick and brittle, and not suitable for the surface functionalization of endovascular catheters [17].

Fibrous protein-based polymers, such as silk, collagen and keratin, are excellent biocompatible candidates with low thermal conductivity on the order of 0.1 W m⁻¹ K⁻¹ [20]. Silk fibroin (SF) is a natural amphiphilic protein and features in a semi-crystalline structure with anti-parallel β -sheet crystalline domains dispersed within a poorly ordered amorphous matrix [21]. The thermal conductivity of SF aerogel

can be as low as $0.026W \cdot m^{-1} \cdot K^{-1}$ [22]. Due to its high structural controllability, the thermal insulation performance of SF can be further enhanced by mixing with other functional materials with high thermal resistance (eg. SF/silica-based composites [23,24]). SF film/coating is appealing to endow the substrate with osteogenetic [25], antimicrobial [26], anticoagulant [27], corrosion-resistant [28], adhesive [29] and drug eluting properties [30]. Nevertheless, its application as biocompatible thermal insulation coatings have not been widely investigated [31]. SF coatings can be formed by using various methods including dip coating, spin coating, electrodeposition and spray coating [30]. Spray coating is a promising technique for surface functionalization of biomedical devices with the advantages of high deposition rate, and controllable coating composition and thickness [32–34]. However, studies on sprayed SF coatings are still in the infant stage [35,36].

In the endovascular setting, the coatings on the catheter should be thin and mechanically robust. Therefore, we designed a novel biocompatible coating with sandwich structures by using dual-sized silica-based hollow-particles as thermal-insulation fillers. The thermal resistant layer was prepared by an air-spraying technique and series of computational models were used to further analyze the parameters influencing their thermal insulation performance. The feasibility of this coating strategy was verified by both of the *in vitro* phantom evaluation and the *in vivo* swine animal model study. The outlet temperature of the cold saline through the coated catheter (75 μm thickness) was approximately 1.8–2.0 °C lower than that of the uncoated one. In summary, this work may facilitate the clinical translation of selective endovascular hypothermia for the neuroprotection in patients with acute ischemic stroke.

2. Materials and methods

2.1. Computational modelling

2.1.1. The modelling of heat transfer across coatings

The influence of geometric parameters of the hollow silica-based particles (HSBP) including diameters and shell thickness on coating thermal conductivity was evaluated by computational modelling and

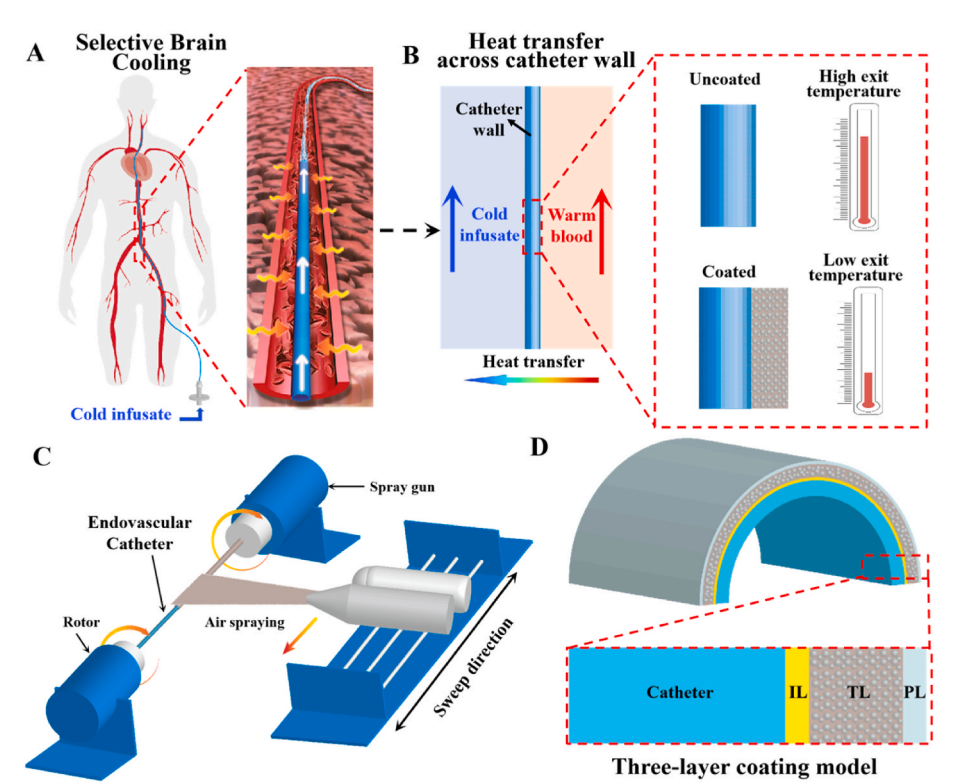


Fig. 1. Selective brain cooling and coating design. An illustration of selective brain cooling by the injection of cold infusate into the catheter from femoral artery to carotid artery (A). The warming effect on the cold infusate within the catheter induced by the heat transfer across catheter wall; and the presence of thermal insulation coatings increases thermal resistance of the catheter walls and results in lower exit temperature (B); schematics of air-spray coating process (C); and the design of three-layer coating model with interfacial layer (IL), thermal insulation layer (TL) and protective sealing layer (PL) (D).

simulations. This simulation was conducted by using COMSOL Multiphysics 6.0 software. Geometry models were built and meshed using tetrahedral element in COMSOL under steady-state heat transfer condition. To decrease the complexity of calculation, we assumed that neighbouring spheres were point contact. The grid numbers were over 2,500,000 for all the models in this simulation. The variables are diameter, shell thickness of HSBP, and thickness of thermal insulation coating. The outer diameters of HSBP were set as 5, 10, 15, 20 μm with 3% shell thickness (shell thickness δ /diameter D), where inner diameters of HSBP can be calculated by $d=D\text{-}2\delta$. Shell thicknesses ratios were set as 1%, 3%, 5%, 10% and 20%.

It was assumed that each HSBP had the same diameter with uniform thickness and smooth surface, with simple cubic packing and point contacting style inside the coatings. To analyze the heat transfer process within the coatings, the upper and lower surfaces of the rectangular coating block were set as the blood temperature ($T_{blood}=310.15~\mbox{K}$) and cold saline temperature ($T_{cold~saline}=277.15~\mbox{K}$) respectively, while the other four surfaces were set as adiabatic. The temperature difference among $120~\mbox{\mu}m$ coating is 33 K. Under such condition when heat transfers from hot side to cold side, the effective thermal conductivity of the model can be expressed according to Fourier's low by following equation [37]:

$$k_{e\!f\!f} = rac{QL}{A\Delta T}$$
 Eq.1

where k_{eff} is the effective thermal conductivity of the simulated block $(W \cdot m^{-1} \cdot K^{-1})$, Q is the total surface heat flow (W), A is the area of upper surface (m^2) , L is the height of block (m) and ΔT is the temperature difference (K) along height L. The total heat flow can be approximated by equation:

$$Q = Q_{HSBN,s} + Q_{rd} + Q_{HSBN,g} + Q_{CV}$$
 Eq.2

Where $Q_{HSBN,s}$ stands for heat conduction of HSBP shell, Q_{rd} for heat transfer by longwave radiation, $Q_{HSBN,g}$ for heat conduction of gas inside HSBP shell and Q_{CV} for heat transfer by gas convection. The radiation and convection effects were neglected in this simulation, because of the relative high extinction coefficient and limited air convection of this structure [38].

The gas molecules inside HSBP were supposed to be presented at an equilibrium state and the Boltzmann equation can be expressed as:

$$\frac{\tau}{\theta} \frac{\partial f}{\partial t'} + \boldsymbol{v'} \cdot \frac{v\tau}{\Lambda} \frac{\partial f}{\partial \boldsymbol{r'}} + \boldsymbol{F'} \cdot \frac{v\tau}{\Lambda} \frac{\partial f}{\partial \boldsymbol{v'}} = -\left[f - f^0\right]$$
 Eq.3

Where f is the velocity distribution function of gas molecular (f^0 the local equilibrium distribution), r is the volume element, v is the velocity, F is the applied external force field, Λ is the mean free path of molecular and τ is the relaxation time. The changes of f are driven by $v\tau/\Lambda$, and hence the Knudsen number of stationary system can be express by:

$$K_n = \frac{l}{\Lambda} = \frac{1}{\sqrt{2n\sigma}} \frac{1}{\Lambda}$$
 Eq.4

Where $n = \frac{p}{k_B T}$ and *l* is the feature size.

The thermal conductivity of air inside the shell can be given by:

$$k_{ai} = \frac{k_a^0}{1 + 2\frac{5\pi}{32} \frac{2-\sigma_T}{\sigma_T} \frac{9\gamma - 5}{\gamma + 1} K n_a}$$
 Eq.5

where k_a^0 is the thermal conductivity of free space air, $\gamma = C_p/C_v$ stands for specific heat capacity ratio, which is 1.4 for diatomic gas molecules, σ_T denotes the thermal accommodation coefficient and it was assumed to be 1 in this calculation, and Kn_a represents the Knudsen number of air. The thermal conductivity of silica shell and silk fibroin were taken as bulk thermal conductivity ($k_{silica} = 1.34 \text{ W/(m·K)}$ [39], $k_{silk \ fibroin} = 0.35 \text{ W/(m·K)}$ [40]).

2.1.2. The modeling of the coatings thermal insulation performance

The coatings thermal insulation performance was analyzed by using ANSYS 17.0 Fluent software to calculate the outlet temperature of saline. A flow model mimicking the actual delivery of cold saline via catheter was built. The catheter was modelled based on the size of Cordis Envoy® MPD 5F catheter with diameter of 1.65 mm (outer) and 1.42 mm (inner). The vessel model was set with a diameter of 6 mm and length of 850 mml. The thicknesses of coatings were set at 0, 30, 75, 120 and 150 μm , and the infusion rate was set at 30 mL/min. The outlet temperatures were plotted against thickness.

2.2. Preparation of thermal insulation coating

2.2.1. Chemicals and reagents

The LiBr, Na₂CO₃, SiO₂, NaOH, NaNO₃, H₃BO₃, dopamine hydrochloride and Tris-HCl buffer solution were purchased from Aladdin Co. Ltd (Shanghai, China). Nylon (PA66) plate, bombyx mori cocoons were purchased from Puhui Zhiyuan Co. Ltd (Beijing, China). The Spray gun (KHOKIA W-71) was used for spray coating. The Cordis Envoy® MPD 5F catheter was utilized as substrate for coatings that used for *in vitro* and *in vivo* animal studies.

2.2.2. Silk fibroin extraction

The fabrication of silk fibroin solution follows the procedure of protocol from Danielle N Rockwood [41]. Firstly, bombyx mori cocoons was cut into pieces and degummed by boiling in $0.02\,M\,Na_2CO_3$ solution for 30 min and dried overnight, followed by dissolution in 9.3 M LiBr solution for 4 h at 60 °C. The resolved liquid was then dialyzed against ultrapure water for 3 days and centrifuged twice to layer silk fibroin solution and impurity. The concentration of silk fibroin solution was diluted to 2 wt% and stored at 4 °C for latter usage.

2.2.3. Hollow glass microspheres preparation

The resulting hollow glass microspheres were prepared using high temperature gas suspension method with the assistance from Gong Yi Van-research Innovation Composite Material Co. Ltd (Zheng Zhou, China). Briefly, the raw materials including silicon dioxide, sodium hydroxide, sodium nitrate, boric acid and dispersant are fully mixed with a high-speed stirrer at 30–80 °C and normal pressure to be prepared as uniform slurry. The slurry was then transported to a spray dryer, and after atomization and rapid dehydration, a HSBP precursor was obtained. The precursor powder was then vitrificated by combustion of natural gas and HSBP of target particle size can be obtained at 700–1100 °C. By adjusting the proportion of raw materials, the softening temperature of the spherical shell can be consistent with the decomposition temperature of nitrate.

2.2.4. Coating process

Materials for spray coating were obtained by adding 1.5 g HSBP and 1 ml glycerol into 10 ml 2 wt% silk fibroin solution. The mixture was then stirred for 15min and filtered to remove denatured silk fibroin, followed by pouring into spray gun. Before the coating process, the PA66 substrates were ultrasonically washed in 70% alcohol and deionized water for 15 min. Both of the PA66 substrates and Cordis Envoy® MPD 5F catheter were surface-activated by immersion into 2 mg/mL dopamine hydrochloride solution in 10 mM Tris buffer (pH = 8.5) for 24 h at room temperature. For better atomization, the spraying pressure was selected as 0.7 MPa and Khokia W-71 spray gun was utilized. To control the spray parameter precisely, a customized rail and a rotor were made to deliver a constant spray distance at 35 cm and sweep speed of 35 mm/ s. Rotational speed of rotor was controlled at 200 rpm. These silk fibroin and HSBP nanocomposite coatings were denoted as TIC (thermal insulation coatings). To further enhance the biocompatibility and integrity of the thermal insulation coating, the resulting samples were further coated by parylene-C using chemical vapor deposition method with the assistance from Zasen Nano tech Co. Ltd (Kun Shan, China) and denoted

as TIC-P (parylene-C modified thermal insulation coatings).

2.3. Morphology and microstructure characterization

The surface morphology of HSBP and coatings were captured using coated Φ 12mm \times 3 mm PA66 discs by scanning electron microscope (SEM; Quanta FEG250) with an accelerated voltage of 20 kV. Since the low electrical conductivity of coatings, all samples were coated with gold. The thickness of coating was measured by analysing SEM images of cross section of coatings using Image Pro Plus software. The microstructural characteristics of the coating were examined by X-ray diffraction (XRD; model) with scan range of 5-90 °at 40 kV. The secondary structure of silk fibroin and the presence of glyceryl and HSBP were analyzed using Fourier Transform Infrared spectroscopic (FTIR; model) performed with range from 600 to 4000 cm⁻¹. To test the adhesion and integration of coatings, a standard tape test was performed according ASTM D 3359-02 [42]. Coatings on $50\text{mm} \times 30\text{mm} \times 3\text{ mm}$ PA66 plates were tested by 3MTM adhesive transfer tape 467 MP and the removal of coatings from the substrate was rated with the scale of 5A-0A.

2.4. Thermal insulation evaluation of coatings

2.4.1. Thermal conductivity characterization

The coatings (TIC and TIC-P) were peeled off from the substrate and then mounted in NETZSCH laser flash analyser 467 to assess thermal conductivity. Parameters of Xenon flash lamp were set as the pulse voltage at 260 V and the pulse width for 150 μ s. The precision and reproducibility of measurement was $\pm 5\%$ and $\pm 3\%$ respectively.

2.4.2. In vitro phantom study

The thermal resistance of the coatings with different thickness was initially evaluated by using a customized rectangular constant temperature water bath to screen out the optimized coating thickness. The Cordis Envoy® MPD 5F catheter was used as the control group. As illustrated in Fig. S1, the cold saline at 4 °C was pumped into interventional catheter soaked in 37 °C water baths. Saline was pumped with infusion rate of 20, 25, 30, 35, 40 mL/min into catheter. The length of catheter immersed into water bath was around 850 mm. The size of water bath is 600 mm in length, 340 mm in width and 260 mm in height. The variation of temperature at inlet and outlet of catheter was monitored by Applent multi-channel temperature meter AT4204 (Changzhou, Jiangsu).

After that, the resulting optimized catheter (TIC-P) and the control group were further analyzed through an in *vitro* artificial circulatory system. This equipment consists of a pulse pump, a temperature control water tank and transparent artificial blood vessels that 1:1 3D printed using silica gel (Fig. S2). The vascular models were filled with 5L/min simulated blood (56% glycerin and 44% DI water, 37 °C) and the 4 °C saline as infusate was injected into this circulatory system through the catheter by an infusion pump at different flow rates of 10–50 mL/min.

2.5. In vitro cytocompatible analysis

2.5.1. Proliferation rate

Human umbilical vein endothelial cells (HUVECs) and human umbilical artery smooth muscle cells (HSMCs) and corresponding Dulbecco's Modified Eagle's Medium (DMEM) were purchased from Procell Co. Ltd (Wuhan, China). Cell Counting Kit-8 was purchased from Millipore-Sigma. The coated PA66 discs were utilized as substrates and the uncoated discs were used as control groups. The extract medium was prepared according to the ISO 10993–5:2009. The samples were incubated with serum-free DMEM with a ratio of 6 cm 2 mL $^{-1}$ in a humidified atmosphere with 5% CO $_2$ at 37 °C for 24 h. HUVECs and HUASMCs were seeded into 24-well plates at a density of 2.0 \times 10 4 cells/well by incubation in DMEM with 10% FBS for 24 h respectively. Then, the medium

in the plates were replaced by the extract and further incubated for 24 h. DMEM medium was exploited as negative control and DMEM medium containing 10% dimethyl sulfoxide was used as positive control. The cell viability was evaluated by CCK-8 assay as mentioned above. Besides, the cells were stained with Hoechst 33342 and Calcein AM, and imaged using an automated microscope.

2.5.2. Inflammatory response

The RAW264.7 cells and corresponding DMEMs were purchased from Procell Co. Ltd (Wuhan, China). LEGENDplexTM multiplex human inflammation panel 1 kit was purchased from Biolegend Co. Ltd. Mouse TGF-betal ELISA kit were purchased from Abcam Co. Ltd. The inflammatory response may happen after intervention of catheter, which may lead to cell hyperplasia and thrombosis. The inflammatory cytokines were measured to study the level of inflammatory reaction. PA66 discs were utilized as substrates and results of bare discs were listed as control. Having incubated for 24 h, the supernatant of macrophages cultured on coatings were collected. The inflammatory cytokines produced by RAW264.7 macrophages after 24 h were measured by ELISA kit. Detected inflammatory cytokines includes two pro-inflammatory cytokines (IL-6 and TNF- α) and one anti-inflammatory cytokine (TGF- β 1).

2.6. In vitro hemocompatible evaluation

2.6.1. Hemolysis test

For this test, fresh human whole blood was taken from volunteers. PA66 discs were utilized as substrates and results of bare discs were listed as control group. Coated discs were soaked in saline solution at 37 $^{\circ}\text{C}$ for 30min and then, adding 0.2 ml diluted cony blood which can be acquired by mixing 5 ml human whole blood with 6.5 ml saline. The sample was then kept at 37 $^{\circ}\text{C}$ for 60min and withdrawn. After the solution was centrifuged at 1000 g for 5 min, the supernatant solution was transferred to a 96-well plate and the optical density (OD) at a wavelength of 545 nm was measured with a spectrophotometer. Finally, hemolytic ratio (HR) can be calculated with equation:

$$HR(\%) = D_t - D_{nc}/D_{pc} - D_{nc} \times 100\%$$
 Eq.6

The D_t stands for absorbance of specimen and D_{nc} is absorbance of negative control (10 ml deionized water with 0.2 diluted cony whole blood) and D_{pc} is absorbance of positive control (10 ml saline with 0.2 diluted cony whole blood).

2.6.2. Fibrinogen (Fg) adsorption

PA66 discs were utilized as substrates and results of bare discs were listed as control. Human fibrinogen ELISA kit was purchased from Abcam Co. Ltd. Fresh human whole blood was acquired from healthy human volunteers, 3.2% trisodium citrate was added with the volume ratio of 1:9 followed by centrifugal for 15 min at 3000 rpm to prepare platelet poor plasma (PPP). 100 μ L PPP was added onto the samples, negative and positive control groups, and incubated for 2 h at 37 °C. Human fibrinogen ELISA kit was utilized to measure adsorbed Fg.

2.7. Animal study

Six adult laboratory miniature swine models (9 month, 45–50 kg) and six 5F Cordis guiding catheters including three TIC-P coated ones were utilized in this experiment. The pigs were divided into two groups, bare catheters group and TIC-P coated catheter group. The swine nasopharyngeal temperature and rectal temperature were measured to represent the cerebral temperature and core body temperature. A temperature-sensor wire was inserted into each catheter from the hub to the distal end and a Y-shaped valve was connected to the hub of catheter to deliver cold saline. Percutaneous catheterization was conducted on the swine models through a femoral artery to common carotid artery

under digital subtraction angiography (DSA) guidance. Cold saline (4 $^{\circ}$ C \pm 2 $^{\circ}$ C) was infused at a rate of 10, 20, 30 and 40 mL/min. Hematoxylin and eosin (HE) staining was performed on common carotid artery. The experiment was designed in accordance with the guideline from the Laboratory Animals Welfare and Ethical Review Board of Capital Medical University of China. And the animal study was performed in Beijing Tonghe Litai Biotechnology Co.Ltd and approved by its Ethical Review Board with support from Beijing Hong Hai Microtech Co., Ltd.

2.8. Statistical analysis

Statistical analysis was performed with Origin software. All data were analyzed using one way analysis of variance (ANOVA) test to determine the significant differences among the groups, and p-values less than 0.05 were considered statistically significant.

3. Result

3.1. Coating design and computational modelling

Selective brain cooling is one kind of therapeutic hypothermia (TH) for neuroprotection by suppressing cerebral oxygen metabolism and energy consumption (Fig. 1A). IA-SCI is considered to be the most effective way for target cooling, and the warming effect on the cold infusate inside the endovascular catheter can reduce its neuroprotective efficiency. To overcome this shortcoming, the addition of thermal insulation coatings can inhibit heat transfer across the catheter wall (Fig. 1B). Previously reported coating techniques, such as spin coating, layer-by-layer and dip-coating, cannot be conveniently exploited onto catheter due to its high length-to-diameter ratio. Therefore, the proposed SF/silica-based composite coatings were prepared by an air spraying technique combined with customized rotatory motors to secure the catheter (Fig. 1C).

Catheter coating composition and thickness can be manipulated to achieve the desired insulation properties. Before the coating process, the substrate should be activated by an interfacial layer to increase the adhesion strength and the stability under blood-flow-induced shear stress. The porous thermal-insulation layer consists of stacked hollow glass particles that are embedded in fibroin matrix. Meanwhile, a protective sealing layer is also designed to prevent the penetration of physiological fluid into the coatings, which is detrimental to their thermal insulation behaviour. Therefore, the heterogeneous thermal resistant coatings were designed to have a three-layer microstructure (Fig. 1D).

Computational modelling of the heat transfer can give insights into the micro structural design of the coatings with high thermal resistance. The HSBPs were assumed to be arranged in a compact cubic packing style by point contact, and the gaps among HSBP were fulfilled with silk fibroin (Fig.2Aa). Besides, contact resistance was ignored in our model. Computational simulations of steady heat transfer were accomplished by the setting upper and lower surfaces as hot (310 K) and cold (277 K) boundaries under standard air pressure. The temperature contour of unit cell in Fig.2Ab,c indicated that heat transfer mainly occurred through silk fibroin and at the contact region of the HSBP shell. According to Eq.7 and Eq.8, the diameter and shell thickness of HSBP may affect the overall thermal conductivity and heat flux of the coatings.

Temperature distribution and total heat flux values along the contour of particles across the coatings were quantitatively presented in detail in Fig.S3. The changes in HSBP diameters (5–20 μ m) exhibited little influence on thermal performance of the coatings with thermal conductivity ranging from 0.28–0.37 W/(m·K). For HSBP (D = 20 μ m), as shell thickness increases from 1% to 20%, thermal conductivity of the coating increases from 0.32 to 0.64 W/(m·K) (Fig.S3D). Notably, heat mainly transfers downward and through the side shells of the particles (Fig.S4).

Therefore, a higher content of silica and lower content of gas leads to an enlargement of overall effective thermal conductivity and total heat flux of the coating. A dual-sized model was developed and fabricated to further enhance the content of HSBP by filling gaps among HSBP with smaller sized HSBP (Fig. 2B). This dual-sized model can further decrease the heat flux values of mono-sized model from 105340 $\mbox{W/m}^2$ to 98625.5 $\mbox{W/m}^2$. Thickness is another critical parameter that influences the thermal insulation performance of the coating. Temperature distribution of the infusate within the catheter obtained by computational simulation was presented in Fig. 2C and indicated that thicker coatings could result in reduced heat loss.

3.2. Preparation and thermal resistance evaluations

The preparation of the sandwich-structured thermal insulation coatings consists of three steps (Fig. 3 A). Firstly, the Cordis Envoy® 5F catheter was surface-activated by polydopamine. Secondly, the mixture of silk fibroin, HSNB and glycerol was air-spray coated onto the substrate. Thirdly, the resulting samples were further coated by parylene-C using the chemical vapor deposition method. HSBP is an excellent thermal insulation filler, with thermal conductivity of 0.020–0.023 W/ (m·K), In this research, a high temperature gas suspension method was exploited to prepare these particles. As shown in Fig.3B and Fig.S5A, the resulting particles displayed intact spherical structures with a wall thickness of 500–600 nm, and their particle size exhibited a bimodal distribution around 5.2 μ m and 21.2 μ m. The Bragg diffraction peak in Fig.S5C at 20 values of 21 °C was indexed to be silica.

The HSBPs were uniformly distributed and embedded within the silk matrix. The presence of parylene-C could fill the gaps and pinholes in TIC, made the stack of HSBPs more compact, and improved the cohesion strength between each HSBP, which was beneficial for the integrity of thermal insulation coating. Two distinctive XRD peaks were detected at $2\theta=8^\circ$ and 22° in Fig.S6A, which corresponded to the α -helix and superposition of β -sheet structures and silica. As for TIC-P coating, an characteristic peak of parylene-C appeared at 14° . The FTIR result in Fig.S6B further confirmed the presence of the coatings. The secondary structure of the SF within the coatings were analyzed by deconvoluting the amide I adsorption peak from 1600 to 1700 cm $^{-1}$ into several subpeaks in Fig.S6C.

The thermal resistant properties of the coatings were initially evaluated in a customized temperature-controlled water tank (Fig.S1). Under the infusion rate of 30 mL/min, the exit temperature gradient between the coatings reached a peak value of 2.5 $^{\circ}\text{C}$ at 75 μm thickness in the ranges of 30–155 μm (Fig. 3C). However, the coating thermalinsulating efficiency was higher for the thin coatings than that of the thick ones. The possible heat transfer process was illustrated in Fig. 3D. As an exception for the ideal scenario, the prepared coatings displayed inferior microstructures with gaps and pinholes, which possibly resulted in blood penetration into the coatings and thus an increase of heat transfer across the catheter wall, especially for thick coatings. Therefore, these air-sprayed coatings were further modified by parylene-C as a capping film using chemical vapor method. The presence of the parylene-C capping film increased the thermal stability of the coatings, and the thermal conductivity of coating is down to 1.05 \times 10 $^{-3}$ W/(m·K) measured by light flash apparatus (Fig.S7C).

During the surgical intervention process, the catheter was subject to bending and rotation, and navigated to pass through curved blood vessels. An insertion of catheter makes an annular gap between the catheter and the vessels, which can increase the wall shear stress induced by the pulsatile blood flow [43]. Therefore, the binding or adhesive strength of the SF/HSBP coatings on the substrate is highly important. Thick coatings are prone to cracking or delamination, and parylene-C modified 75 μm coatings (TIC-P) were utilized in the following study. The tape test in Fig.S8A demonstrated an acceptable adhesive strength of the coatings. The coated catheter could be smoothly inserted in the vascular models and no peeling or cracking was observed on the coatings under bending and rotational scenarios Fig.S8 B,C, which demonstrated comparable flexibility with the pristine catheter.

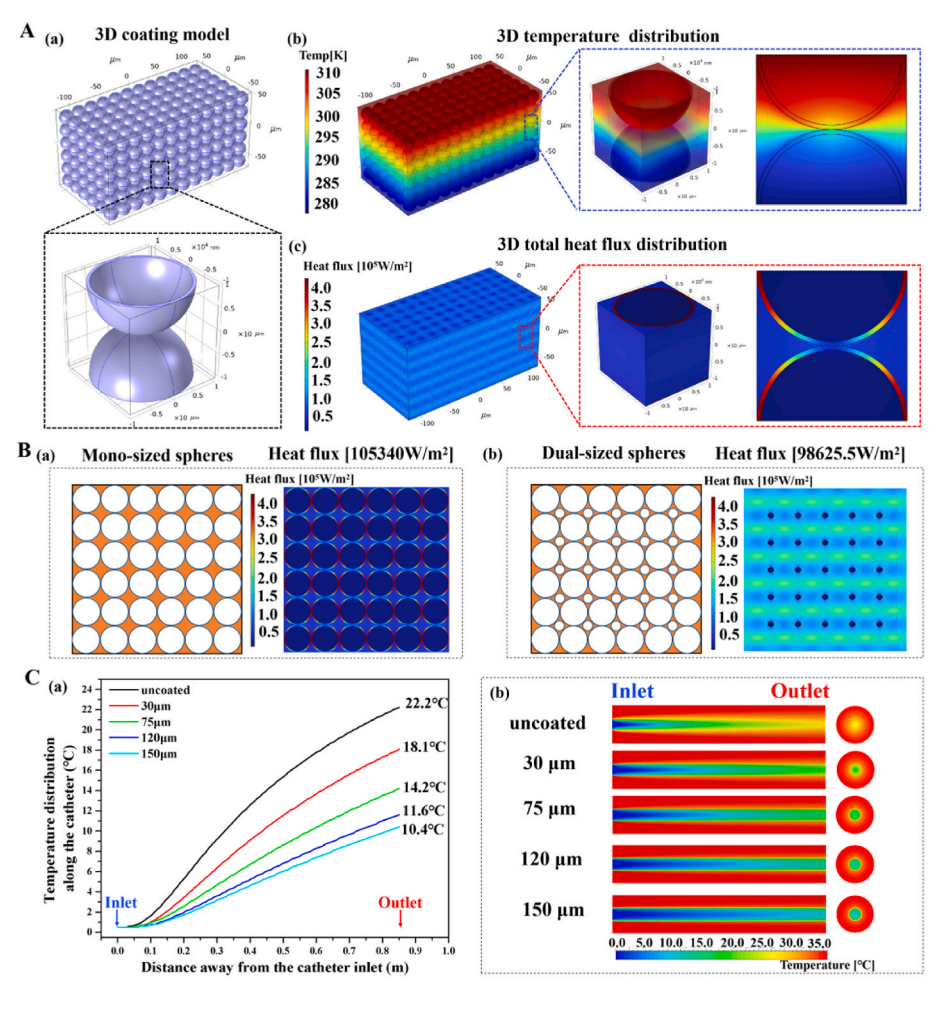


Fig. 2. Thermal modelling of the heat transfer across the coatings. The schematic illustration of the coating model (a); temperature distribution (b) and contours of total heat flux (c) of a packing unit within the coatings (A). The illustration of the porous structure of the coatings by using mono-sized (a) and dual-sized hollow spheres (b), as well as the corresponding heat flux value (B). Numerical simulation of the temperatures (a) and the two-dimensional temperature distributions (b) along the catheter with different coating thickness at a infusion rate of 30 mL/min(C).

3.3. The in vitro phantom study

An artificial circulatory system was used to better evaluate the thermal insulating property of the coatings. This equipment consists of a pulse pump, a temperature-controlled water tank and transparent artificial blood vessels that are 3D-printed using silica gel (Fig. 4A and Fig. S2). A temperature sensor wire was inserted into the catheter to measure the outlet temperature (Fig.4Ba) and the catheter was inserted from the femoral artery (Fig.4Bb) to the aortic arch (Fig.4Bc), and all the way up to the common carotid artery (Fig.4Bd)) to perform the *in vitro* selective brain cooling operation. Outlet temperature of the perfusate at the distal tip of the catheter (T_2) and temperature at the middle cerebral artery (MCA) of the artificial vascular systems (T_3) were monitored by a thermocouple T-type multi-channel temperature sensor (Fig. 4C).

The results showed that a higher infusion rate resulted in faster cooling rate and lower exit temperature. The temperature discrepancy therein at different flows were 2.1 °C (10 mL/min), 1.8 °C (20 mL/min), 1.7 °C(30 mL/min), 1.4 °C (40 mL/min) and 1.3 °C(50 mL/min). The in vitro experiment suggested that the warming effects on the cold fluid within the catheter were much higher under low flow rates and the changes of temperature at the MCA displayed a similar trend. During the selective cooling infusion process, the arc temperature under different infusion flow rates remained stable. Compared with the uncoated catheter, the coated catheter displayed higher cooling capacity, and could potentially cool the brain to target temperature by using a lower volume of infusate with lower dilution rate of hematocrit (HCT), especially under a low infusate rate.

3.4. In vitro cytocompatible and hemocompatible evaluation

The biocompatibility of the coatings was evaluated by in vitro indirect contact method according to ISO standard. The HUVECs and HSMCs were cultured with the extraction media of the coatings for 24 h and their morphologies were evaluated by immunofluorescence staining (Fig. 5A). During the cooling infusion process, the catheter is inserted through the blood vessels. Both of the HUVEC and HSMC displayed healthy morphologies, and compared with TIC, the TIC-P group showed a higher proliferation rate. Apart from vessel cells, its influence on immune cells is also crucial. Macrophages, as an important type of immune cells, are involved in inflammatory response to tissue injury caused by interventional surgery. After incubation for 24 h, the proliferation rate of RAW 264.7 cells in TIC-P was higher than that of the TIC group. The phenotype of macrophages was investigated by detection of inflammatory cytokine expression IL-6 and TNF-α, as well as the antiinflammatory factors TGF- β1. These factors were detected by using an inflammation panel kit in the supernatants of Raw 264.7 macrophages incubated on coatings. As shown by Table. S1, the result indicates that all coatings will not induce inflammatory response of macrophages. As shown in Fig. 5C, the coatings showed low hemolysis index. The change of composition didn't have a significant influence on hemolysis index. Adsorption and activation of fibrinogen played a key role in response of platelets to materials. The degree of activation of fibrinogen of different coatings was also similar. TIC-P coatings had equivalent hemocompatibility compared with TIC coating.

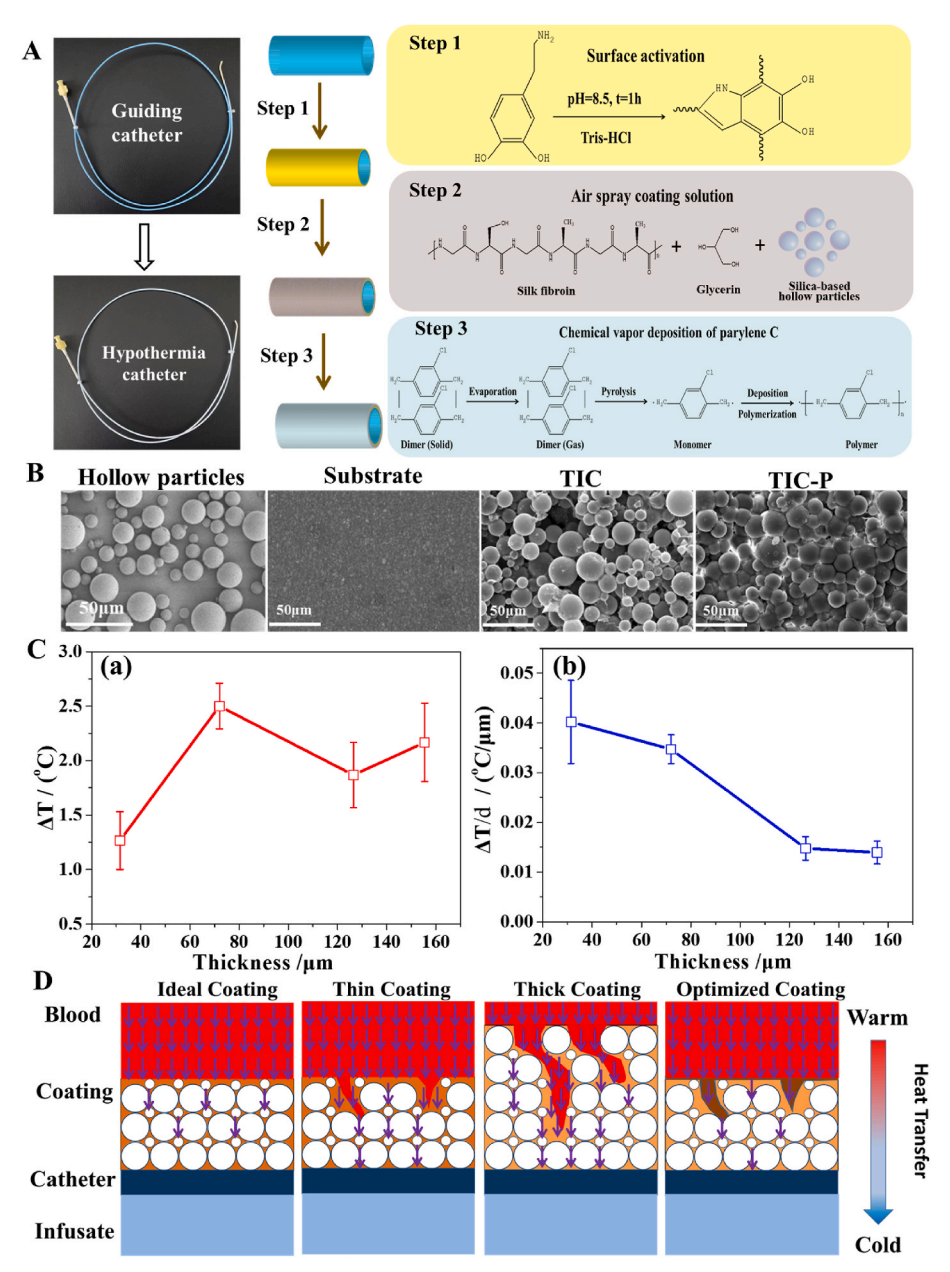


Fig. 3. Schematic diagram of the coating process, morphology characterization and thermal resistance evaluation. Optical photos of the pristine (upper panel) and coated catheters (lower panel); The three-layered structures of the coatings prepared by surface activation through dopamine polymerization (step 1), air spraying (step 2) and chemical vapor deposition of parylene-C (step 3) (A); SEM images of the prepared HSBP as well as the surface morphology of the substrate, TIC and TIC-P coatings (B); The exit temperature differences between the uncoated and coated catheters with different coating thickness through *in vitro* studies (C); and the illustration of the heat transfer process through different coatings (D).

3.5. Animal study

Selective endovascular cerebral hypothermia was conducted on six swine models by using TIC-P and uncoated catheters. 200 mL cold saline (4 \pm 0.1 °C) was infused at a rate of 30 mL/min through the pathway shown in Fig. 6Aa. Anesthesia and ventilation were performed during the study, and the heart rate and blood pressure in the swine model were also monitored. Before the cooling process, cerebral angiography was performed to ensure the right position of the catheter, and the liquid was successfully injected into the swine brain (Fig. 6B). The catheter exit temperature dropped greatly during the first 20s of infusion and stabilized after 60s. Compared with the uncoated catheter, the plateau temperature of the TIC-P group was approximately 2 $^{\circ}\text{C}$ higher than that of the control group. The tympanic temperature of the swine using the TIC-P catheter dropped down to 30 °C during the infusion and increased to around 33 °C. Both of the contralateral tympanic and rectal temperatures showed minor fluctuations, which confirmed that selective brain cooling has a great potential to circumvent the side effects of wholebody cooling (Fig.S9). The HE staining of the CCA vessels further

confirmed the tissue-compatibility of the TIC-P coatings and the images at larger magnification were presented in Fig.S10. In terms of cooling efficiency, the TIC-P catheter was higher than the uncoated 5F guiding catheter, and compared with the other studies, the TIC-P catheter displayed faster cooling efficiency by using a low volume of infusate.

4. Discussion

Selective brain cooling was considered as the most promising hypothermic neuroprotective method for AIS treatment. Even though the brain accounts for 2% of the total body weight in humans, it consumes 20%–25% of the resting metabolism; and the high level of cerebral blood flow greatly counteracts the cooling effects of the AIS and results in rewarming of the brain tissue. Therefore, direct cooling on the brain through IA-SCI displays superior neuroprotective efficiency than other hypothermia methods. Among all the hypothermic methods, IA-SCI can provide faster target cooling rate. This result has been confirmed by rat, swine, dog and monkey studies [44]. Regional cerebral infusion was also performed on patients with AIS through a microcatheter in three clinical

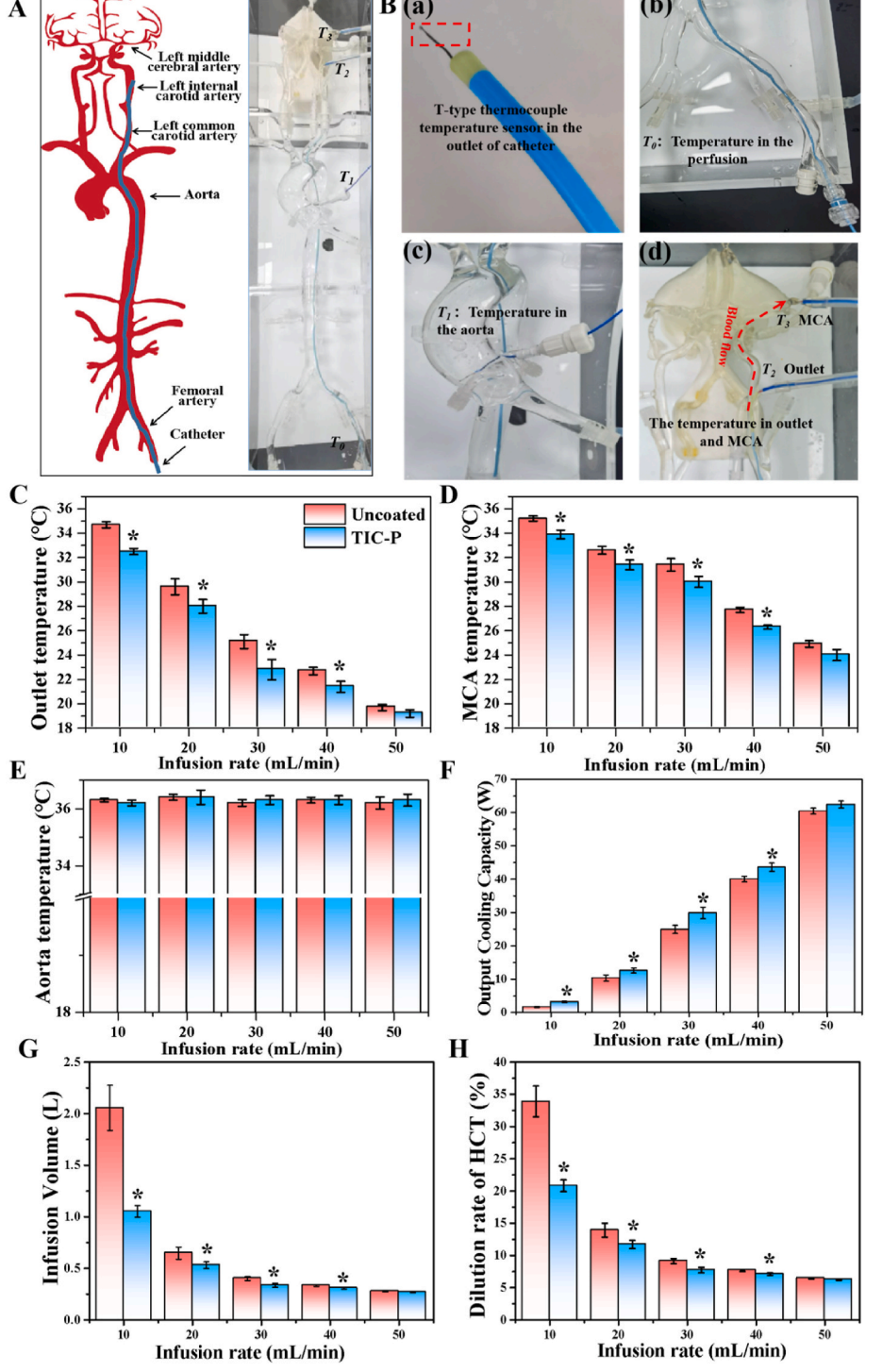


Fig. 4. The *in vitro* evaluation of the cooling performance of thermal insulated catheter. Schematic illustration of the 1:1 simulated blood vessels and the insertion pathway (A); the picture of the temperature sensor at the catheter outlet (a); the perfusate temperature in perfusion as T_0 (b), aorta as $T_1(c)$, catheter outlet as T_2 and MCA as T_3 (d). The comparison of the infusate temperatures by using coated and uncoated catheters at outlet (C), MCA (D), aorta (E) as well as their output cooling capacity (F) at infusion volume rate from 10 mL/min to 50 mL/min; the infusion volume required to target brain cooling temperature (G) and the related dilution rate of HCT (H) were presented. * represents p < 0.05 (compared with the uncoated group).

trials, and infarct volumes of the hypothermia group were significantly reduced compared with the control group by using an infusion rate of 30–33 mL/min [14,45,46]. The thrombectomy for AIS patients via the femoral artery is a standard procedure within neurosurgery. In a small subset of patients, direct carotid puncture can be conducted as an alternative approach, but with risks of carotid artery dissection and neck hematomas [47]

During IA-SCI, the rate and duration of brain cooling was volumedependent and the elevated catheter exit temperature may potentially require the administration of a larger fluid volume, which may cause systemic or local hemodilution and increase the risk of hemorrhagic transformation [48]. Computational models have been proposed to predict the cerebral cooling effects of IA-SCI on stroke patients. Slotboom et al. [8,49] indicated that the infusion of 15 °C 15 mL/min saline can cool the 300 g ischemic brain tissue below 34 °C within 6 min; and Konstas et al. [50] proposed that 150 mL cold liquid can decrease the penumbra temperature down to 34 °C within 6 min. However, one limitation of those numerical models is the assumption that the cold fluid was injected through a thermally insulated catheter. This is different from current clinical practice and also cannot induce the desired local hypothermia. As a result, the design of thermal insulating catheter can offer a faster cooling rate by using a relatively low volume

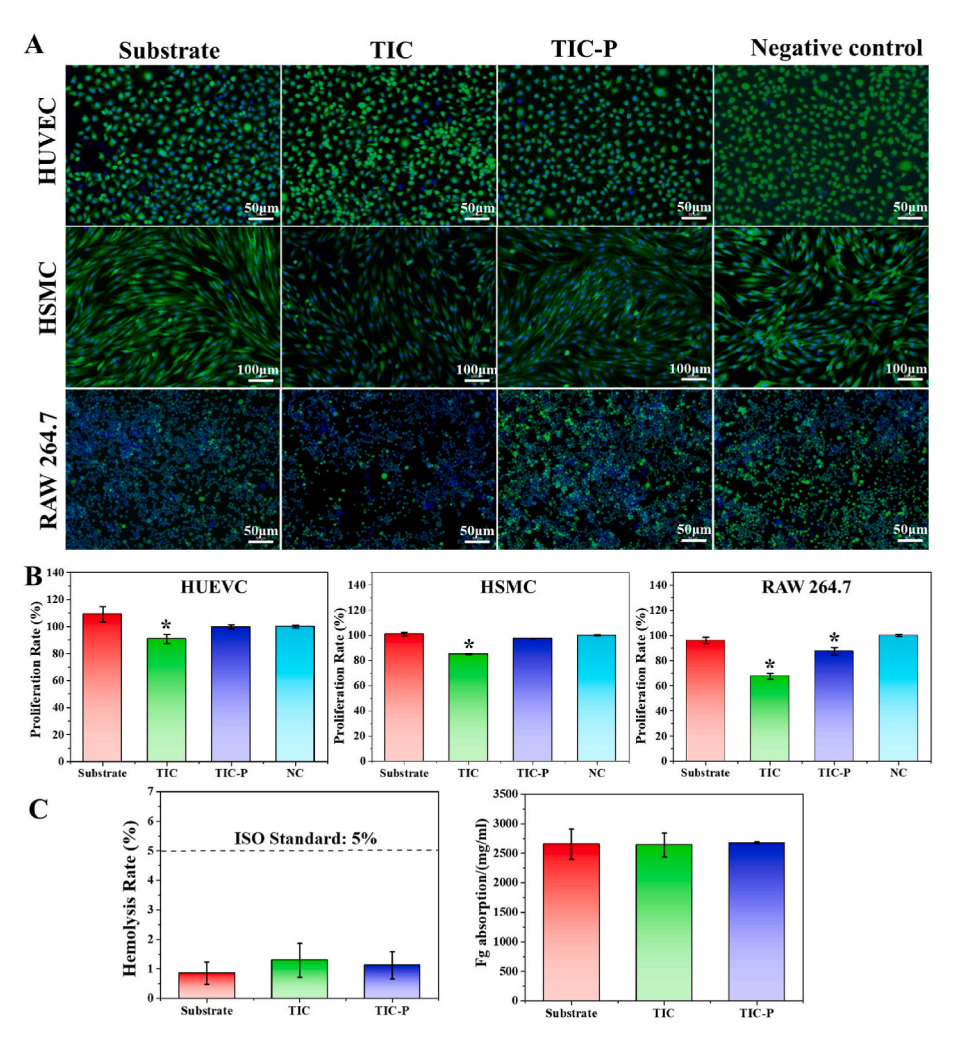


Fig. 5. *In vitro* biocompatible analysis of the samples. The immunofluorescence images of HUVEC, HSMC and RAW 264.7 cells after being cultured in the extraction media of the samples for 24 h (A) as well as their proliferation rate (B). The blood compatible evaluation of the samples was conducted by hemolysis rate and Fg absorption analysis (C). * represents p < 0.05 (compared with the NC group).

of cold infusate (Fig. 6E).

Surface engineering remains a crucial technique in improving functionality of biomaterials. In our study, a thermal insulation coating was successfully fabricated on a catheter with good mechanical property and biocompatibility. The fibroin/silica-based heterogenous coatings with dual-sized-hollow-microparticle incorporated structures were prepared by an air spraying technique. Except for its low thermal conductivity, SF was considered to be a promising medical adhesive [51], which is originated from amino acid side chains through coordinate (dative) bond or hydrogen bond formation (such as serine and tyrosine). The abundant hydrogen bonds within or between HSBP and SF contribute to the enhancement of the cohesive strength of the coating. The SF/HSBP nanocomposite coatings were previously prepared by different spray parameters and coating solution compositions to identify the optimum conditions for coating integrity and adhesion strength [31]. Both modelling and experimental studies suggested that thicker coatings could result in higher thermal resistance with lower exit temperatures. However, thick coatings are prone to cracking or delamination; especially under the force of bending and rotation. Therefore, sandwich-structured thermal insulating coatings were proposed. During the coating fabrication process, the catheter was first surface-activated by the polymerization of dopamine; the catechol therein provides robust and durable adhesion strength to the catheter substrate surfaces and contributes to an increase in adhesive strength [52]. Then the coatings were functionalized by chemical vapor deposited parylene-C

coatings, which are extremely conformal and utilized as flexible protecting encapsulation film [53]. The *in vitro* biocompatibility studies suggested that the resulting coatings have low hemolysis rate, and low cytotoxicity and inflammatory response. This indicates that thermal insulation coating can be a competitive candidate for surface functionalization of interventional catheters. And other biopolymers, such as collagen and keratin, may be considered as an alternative to silk as thermal resistant matrix [20]. Moreover, the silk fibroin could be also chemically modified by dopamine to increase the adhesion and cohesion strength of the coatings.

To obtain a deeper understanding of the heat transfer process within the coatings, computational modelling was conducted. Its overall thermal conductivity mainly consists of two parts, binder matrix (silk fibroin) and distributed particles (HSBP), which can be calculated from equation derived by Hamilton et al. [54]:

$$\frac{k_{Coating}}{k_{SF}} = \frac{[k_{HSBP} + (n-1)k_{SF} - \nu_{HSBP}(n-1)(k_{SF} - k_{HSBP})]}{[k_{HSBP} + (n-1)k_{SF} + \nu_{HSBP}(k_{SF} - k_{HSBP})]}$$
(Eq.7)

where $k_{Coating}$, k_{HSBN} , k_{SF} stand for thermal conductivities of thermal insulation coating, HSBP and SF respectively; k_{HSBN} is much lower than k_{SF} ; v_{HSBN} is the volume fraction of HSBP; n refers to parameter related to particle shape and equals to 3 when thermal conductivity of HSBP is lower than that of SF. This equation was validated with volume fraction lower than 30% by Hamilton [54], and Kiil showed that this equation is also acceptable for higher volume fraction for no binder-intruded

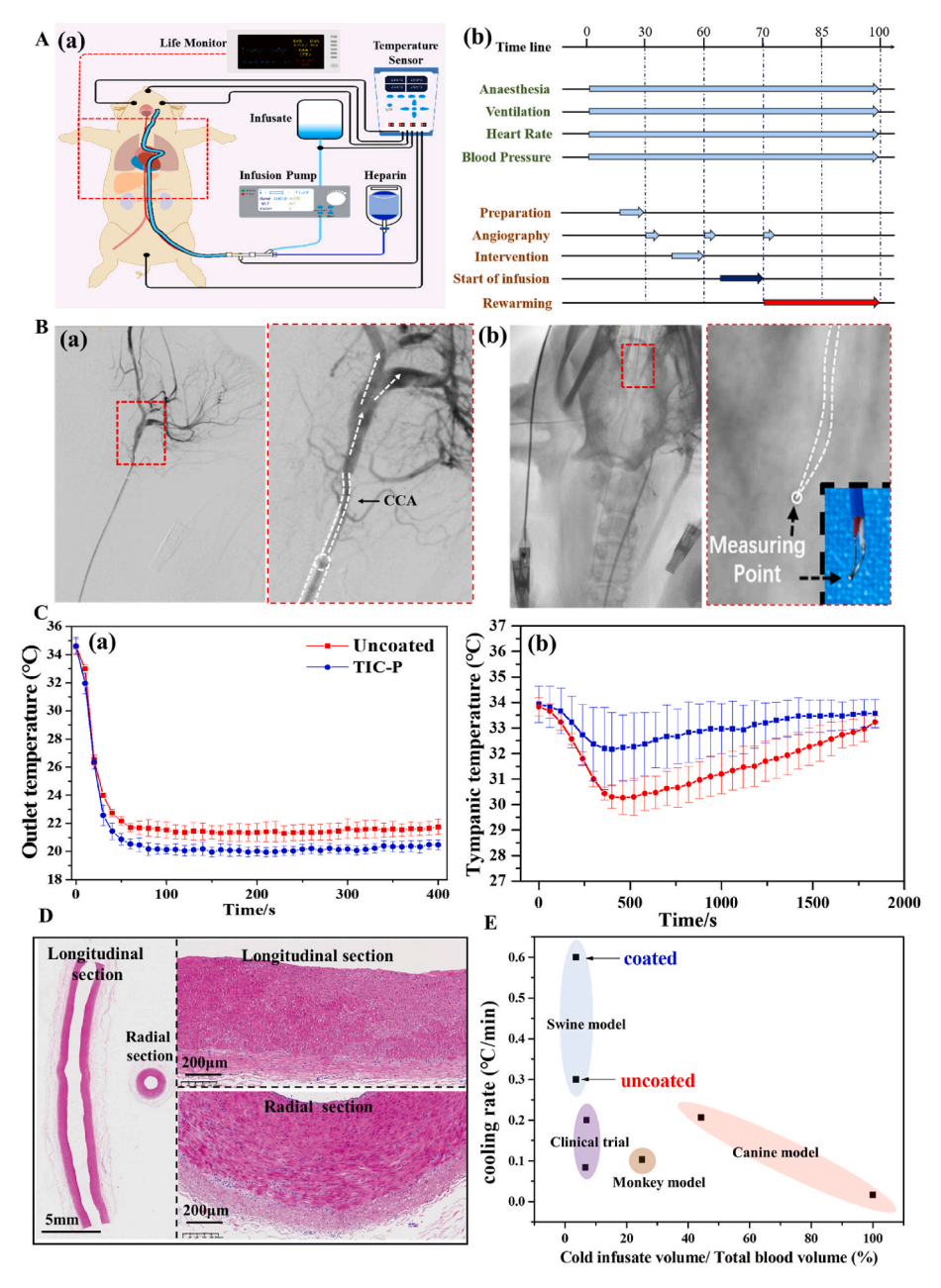


Fig. 6. Animal study results. The equipment setup of selectively endovascular hypothermia on swine model (a) and the timeline for each process (b) (A). The catheter was inserted into CCA (a) and nasopharyngeal temperature was detected by inserting the sensor into the pig nose as brain temperature (b) (B). The variation of saline outlet temperature (a) and tympanic temperature (b) along the cooling process were monitored (C). HE staining of CCA vessel (D). The summary and analysis of several selective brain cooling study results on swine, canine and monkey models, as well as two clinical trials; and the related references were listed in Table S2(E). The CCA is short for common carotid artery.

particles [55]. It can be observed that increasing the volume fraction of HSBP is beneficial for decreasing the thermal conductivity of coating.

Although the maximum and minimum values of total heat flux are different, the fluctuation in the thermal conductivity of the coatings is relatively small, ranging from 0.25 to 0.37 (W/(m·K)). As all HSBPs are micro-level, the total heat flux of coating consists of heat flux of gas inside HSBP, HSBP shell and silk fibroin outside. Constant thickness ratio indicates the same content of gas, HSBP shell and silk fibroin, which indicates an unchanged heat flux between each item. Consequently, for thermal insulation coatings fabricated with micro-level HSBP, the variation of HSBP diameter didn't show an significant effect on the thermal conductivity of coatings. The thermal resistance can be expressed by

$$R = L/Ak$$
 (Eq.8)

Where L, A, k refer to thickness, perpendicular area to direction of heat flow, and thermal conductivity. The heat flow of catheter wall can be calculated by:

$$q = [(T_1 - T_2) Ak] / L$$
 (Eq.9)

Where T_1 , T_2 represents the temperature of flow outside and inside catheter.

The computational modelling and experimental simulation tests showed that the designed coatings displayed an outstanding thermal insulation performance and were able to decrease the outlet temperature of cold infusate at distal end effectively. Furthermore, compared with a single size of HSBP (D = 20 μm), coatings containing HSBP with two kinds of diameters (D = 5 μm and D = 20 μm) have lower thermal conductivity (0.33 W/(m·K) v.s. 0.37 W/(m·K)). Since small HSBP can occupy the gaps between large HSBP, this increases the air volume fractions within the coatings with enhanced thermal resistance.

The thermal insulation behavior of the coating was initially demonstrated through a temperature-controlled water tank (Fig.S1). This finding is roughly in line with our numerical studies that thicker coating and faster infusion rate would result in a lower exit temperature. We reach a balance of thermal resistant efficiency, coating thickness and

mechanical integrity by using parylene-C modified 75 μ m coatings. The reported theoretical calculations indicate that infusions at a rate of 30 mL/min could be sufficient for rapid brain cooling [50]. Under this infusion rate, the outlet temperature of the coated catheter was 1.8–2.0 °C lower than that of the uncoated one, which was also verified thorough an artificial circulatory system (Fig. 4A).

The catheter's potential for in *vivo* application was evaluated under real-world scenarios by using a healthy swine model. Both of the uncoated and TIC-P catheters were inserted from the femoral artery, and can be easily maneuvered through aorta and navigated all the way up to the brain. Tympanic temperatures of the swine models decreased from 34 °C down to 32 °C and 30 °C respectively (Fig.6Cb). The neuroprotective efficiency of the hypothermia treatment was temperature-dependent [56], which was considered to take effect primarily by lowering brain metabolism (1 °C decrease in brain temperature results in a 6% reduction in cerebral metabolic rate) [57]. The stroke animal models will be utilized in the future study.

This proof-of-concept study shows the viability of making a thermal insulating catheter dedicated for selective brain cooling, and may spark further investigations in related temperature-sensitive therapies. On the other hand, our thermal-insulating coating technique may show great potentials to keep warm fluid within the catheter from cooling, which can be used for maintaining a high body temperature in intensive care unit or operating room [58]. In terms of intraperitoneal hyperthermic perfusion for the treatment of cancers, the accurate control of the catheter outflow is also crucial to ensure the safety and efficacy of the therapy [59].

5. Conclusion

In summary, we designed and fabricated a silica-based hollow microparticle incorporated fibroin thermal insulation coating on a commercially available guiding catheter for therapeutic cerebral hypothermia. The functionalized catheter exhibited better performance than the uncoated one in terms of cooling efficiency, which may facilitate the clinical translation of selective endovascular hypothermia for the neuroprotection in patients with acute ischemic stroke.

Ethics approval and consent to participate

The experiment was designed in accordance with the guideline from the Laboratory Animals Welfare and Ethical Review Board of Capital Medical University of China. And the animal study was performed in Beijing Tonghe Litai Biotechnology Co.Ltd and approved by its Ethical Review Board with support from Beijing Hong Hai Microtech Co., Ltd.

CRediT authorship contribution statement

Ming Li: Conceptualization, Data curation, Writing – original draft. Yuan Gao: Methodology, Software, Formal analysis, Investigation, Writing - original draft. Miaowen Jiang: Methodology, Software, Formal analysis, Investigation, Writing - original draft. Hongkang Zhang: Methodology, Investigation. Yang Zhang: Methodology, Investigation. Yan Wu: Methodology, Investigation. Wenhao Zhou: Writing - review & editing. Di Wu: Writing - review & editing. Chuanjie Wu: Writing - review & editing. Longfei Wu: Writing - review & editing. Luzi Bao: Methodology, Investigation. Xiaoxiao Ge: Writing - review & editing. Zhengfei Qi: Visualization. Ming Wei: Visualization. Ang Li: Writing - review & editing. Yuchuan Ding: Writing - review & editing. Jicheng Zhang: Resources. Guangzhen Pan: Resources. Yu Wu: Resources. Yan Cheng: Conceptualization, Supervision, Funding acquisition. Yufeng Zheng: Conceptualization, Supervision, Funding acquisition. Xunming Ji: Conceptualization, Supervision, Funding acquisition.

Declaration of competing interest

We declare that we have no known competing financial interests or personal relationships that could have appeared to influence the work reported in this paper.

Acknowledgement

This work was supported by National Natural Science Foundation of China (82102220, 82027802, 61975017, 82071468), Beijing Municipal Science and Technology Commission (Z221100007422023), General Projects of Scientific and Technological Plan of Beijing Municipal Education Commission (KM202010025023), and Talents Gathering Project of Xuanwu Hospital Capital Medical University.

Appendix A. Supplementary data

Supplementary data to this article can be found online at https://doi.org/10.1016/j.bioactmat.2023.02.022.

References

- V.L. Feigin, G. Nguyen, K. Cercy, C.O. Johnson, G.A. Roth, Global, regional, and country-specific lifetime risks of stroke, 1990 and 2016, N. Engl. J. Med. 379 (25) (2018) 2429–2437.
- [2] V. Saini, L. Guada, D.R. Yavagal, Global epidemiology of stroke and access to acute ischemic stroke interventions, Neurology 97 (20 Suppl 2) (2021) 6–16.
- [3] D. Wu, M. Li, M. Fisher, X. Ji, Brain cytoprotection of ischemic stroke in the era of effective reperfusion, Sci. Bull. 67 (23) (2022) 2372–2375.
- [4] M. Goyal, B.K. Menon, W.H. van Zwam, D.W. Dippel, P.J. Mitchell, A.M. Demchuk, A. Davalos, C.B. Majoie, A. van der Lugt, M.A. de Miquel, G.A. Donnan, Y.B. Roos, A. Bonafe, R. Jahan, H.C. Diener, L.A. van den Berg, E.I. Levy, O.A. Berkhemer, V. M. Pereira, J. Rempel, M. Millan, S.M. Davis, D. Roy, J. Thornton, L.S. Roman, M. Ribo, D. Beumer, B. Stouch, S. Brown, B.C. Campbell, R.J. van Oostenbrugge, J. L. Saver, M.D. Hill, T.G. Jovin, Endovascular thrombectomy after large-vessel ischaemic stroke: a meta-analysis of individual patient data from five randomised trials, Lancet (London, England) 387 (10029) (2016) 1723–1731.
- [5] X. Xiao-Yi, L. Liang, Y. Qing-Wu, Refocusing neuroprotection in cerebral reperfusion era: new challenges and strategies, Front. Neurol. 9 (2018) 249.
- [6] J.M. Hong, E.S. Choi, S.Y. Park, Selective brain cooling: a new horizon of neuroprotection, Front. Neurol. 13 (2022), 873165.
- [7] E. Esposito, M. Ebner, U. Ziemann, S. Poli, In cold blood: intraarteral cold infusions for selective brain cooling in stroke, J. Cerebr. Blood Flow Metabol. 34 (5) (2014) 743–752.
- [8] J. Slotboom, C. Kiefer, C. Brekenfeld, C. Ozdoba, L. Remonda, K. Nedeltchev, M. Arnold, H. Mattle, G. Schroth, Locally induced hypothermia for treatment of acute ischaemic stroke: a physical feasibility study, Neuroradiology 46 (11) (2004) 923–934.
- [9] A.A. Konstas, M.A. Neimark, A.F. Laine, J. Pile-Spellman, A theoretical model of selective cooling using intracarotid cold saline infusion in the human brain, J. Appl. Physiol. 102 (4) (2007) 1329–1340.
- [10] T.L. Merrill, J.E. Mitchell, D.R. Merrill, Heat transfer analysis of catheters used for localized tissue cooling to attenuate reperfusion injury, Med. Eng. Phys. 38 (8) (2016) 758–766.
- [11] B. Ajaa, B. Bee, C. Mtc, An investigation of effect of hematocrit on thermal conductivity of a bio-nanofluid (MWCNT or SWCNT with blood), Therm. Sci. Eng. Prog. 25 (2021), 100985.
- [12] T. Merrill, J. Mitchell, D. Merrill, Heat transfer analysis of catheters used for localized tissue cooling to attenuate reperfusion injury, Med. Eng. Phys. 38 (8) (2016) 758–766.
- [13] T.L. Merrill, B.F. Smith, J.E. Mitchell, D.R. Merrill, B.A. Pukenas, A.A. Konstas, Infusion warm during selective hypothermia in acute ischemic stroke, Brain Circul. 5 (4) (2019) 218.
- [14] J.H. Choi, R.S. Marshall, M.A. Neimark, A.A. Konstas, E. Lin, Y.T. Chiang, H. Mast, T. Rundek, J.P. Mohr, J. Pile-Spellman, Selective brain cooling with endovascular intracarotid infusion of cold saline: a pilot feasibility study, Ajnr Am. J. Neuroradiol. 31 (5) (2010) 928–934.
- [15] G. Cattaneo, M. Schumacher, J. Wolfertz, T. Jost, S. Meckel, Combined selective cerebral hypothermia and mechanical artery recanalization in acute ischemic stroke: in vitro study of cooling performance, Am. J. Neuroradiol. 36 (11) (2015) 2114–2120.
- [16] T.K. Mattingly, D.M. Pelz, S.P. Lownie, Cooling catheters for selective brain hypothermia, Ajnr Am. J. Neuroradiol. 37 (5) (2016) E45.
- [17] B. Abu-Jdayil, A.H. Mourad, W. Hittini, M. Hassan, S. Hameedi, Traditional, state-of-the-art and renewable thermal building insulation materials: an overview, Construct. Build. Mater. 214 (2019) 709–735.
- [18] Y. Pan, Research progress and application status of thermal insulation coatings, IOP Conf. Ser. Earth Environ. Sci. 295 (3) (2019), 032048.

- [19] D. Chellaganesh, M.A. Khan, J. Jappes, Thermal barrier coatings for high temperature applications – a short review, Mater. Today Proc. 45 (2020) 1529–1534.
- [20] Y. Xue, S. Lofland, X. Hu, Thermal conductivity of protein-based materials: a review, Polymers 11 (3) (2019) 456.
- [21] T.P. Nguyen, Q.V. Nguyen, V.H. Nguyen, T.H. Le, Q.V. Le, Silk fibroin-based biomaterials for biomedical applications: a review, Polymers 11 (12) (2019) 1933.
- [22] H. Maleki, M. S., H.-R. N., P. F., H. N., Compressible, thermally insulating, and fire retardant aerogels through self-assembling silk fibroin biopolymers inside a silica structure-an approach towards 3D printing of aerogels, ACS Appl. Mater. Interfaces 10 (26) (2018) 22718–22730.
- [23] Z. Xin, C. Zhuoyue, L. Yuxiao, H. Qian, Z. Huidan, Silk fibroin microparticles with hollow mesoporous silica nanocarriers encapsulation for abdominal wall repair, Adv. healthcare mater. 7 (21) (2017), 1801005.
- [24] Y. Cheng, G. Cheng, C. Xie, C. Yin, Z. Li, Biomimetic silk fibroin hydrogels strengthened by silica nanoparticles distributed nanofibers facilitate bone repair, Adv. Healthcare Mater. 10 (9) (2021), e2001646.
- [25] W. Zhou, Z. Jia, X. Pan, J. Yan, Y. Zheng, Bioinspired and biomimetic AgNPs/gentamicin-embedded silk fibroin coatings for robust antibacterial and osteogenetic applications, ACS Appl. Mater. Interfaces 9 (31) (2017) 25830–25846.
- [26] M. Pranothi, K. Deep, H. Raquib, Q. Mohiuddin, Y. Wang, B. Amanda, Development and processing of novel heparin binding functionalized modified spider silk coating for catheter providing dual antimicrobial and anticoagulant properties - ScienceDirect, Materialia 14 (2020), 100937.
- [27] S. Tomoko, S. Yu, A. Derya, T. Ryou, A. Tetsuo, In vitro and in vivo evaluation of hemocompatibility of silk fibroin based artificial vascular grafts, Int. J. Chem. 6 (2) (2014) 1-14
- [28] X. Wei, Y. Kai, T. Asakura, M. Sasaki, T. Niidome, Silk fibroin as a coating polymer for sirolimus-eluting magnesium alloy stents, ACS Appl. Bio Mater. 3 (1) (2019) 531–538.
- [29] X. Liu, J. Liu, J. Wang, T. Wang, J. Yu, Bio-inspired, micro-structured silk fibroin adhesives for flexible skin sensors, ACS Appl. Mater. Interfaces 12 (5) (2020) 5601–5609
- [30] C.B. Borkner, M.B. Elsner, T. Scheibel, Coatings and films made of silk proteins, ACS Appl. Mater. Interfaces 6 (18) (2014), 15611.
- [31] G. Yuan, J. Miaowen, B. Luzi, Y. Zhichen, Z. Jicheng, P. Guangzhen, Z. Shiqiang, Z. Yufeng, W. Chuanjie, L. Ming, J. Xunming, Preparation and characterization of air sprayed silk fibroin/silica-based thermal-insulation coatings on catheters for cerebral hypothermia therapy, Surf. Innov. 11 (2023) 155–168.
- [32] E.A. Turner, M.K. Atigh, M.M. Erwin, U. Christians, S.K. Yazdani, Coating and pharmacokinetic evaluation of air spray coated drug coated balloons, Cardiovascul, Eng. Technol. 9 (2018) 240–250.
- [33] S. Srisang, N. Nasongkla, Spray coating of foley urinary catheter by chlorhexidine-loadedpoly(e-caprolactone) nanospheres: effect of lyoprotectants, characteristics, and antibacterial activity evaluation, Pharmaceut. Dev. Technol. 24 (4) (2018) 402–409.
- [34] M.H. Kang, K.H. Cheon, K.I. Jo, J.H. Ahn, T.S. Jang, An asymmetric surface coating strategy for improved corrosion resistance and vascular compatibility of magnesium alloy stents, Mater. Des. 196 (2020), 109182.
- [35] C. Liu, J. Li, L. Che, S. Chen, X. Zhou, Toward large-scale fabrication of triboelectric nanogenerator (TENG) with silk-fibroin patches film via spray-coating process, Nano Energy 41 (2017) 359–366.
- [36] J. Yang, J. Chen, Y. Hao, Y. Liu, Identification of the DPPH radical scavenging reaction adducts of ferulic acid and sinapic acid and their structure-antioxidant activity relationship, LWT- Food Science and Technology. (1–2) (2021), 111411.
- [37] O. Khayal, Fundamentals of Heat and Mass Transfer, 2017.
- [38] G. Wei, Y. Liu, X. Zhang, F. Yu, X. Du, Thermal conductivities study on silica aerogel and its composite insulation materials, Int. J. Heat Mass Tran. 54 (11) (2011) 2355–2366.

- [39] H. Liu, M. Hu, J. Jiao, Z. Li, X. Wu, Effective thermal conductivity modeling of hollow nanosphere packing structures, Int. J. Heat Mass Tran. 161 (2020), 120298.
- [40] S. Xu, Z. Xu, J. Starrett, C. Hayashi, X. Wang, Cross-plane thermal transport in micrometer-thick spider silk films, Polymer 55 (7) (2014) 1845–1853.
- [41] D.N. Rockwood, R.C. Preda, T. Yucel, X. Wang, M.L. Lovett, D.L. Kaplan, Materials fabrication from Bombyx mori silk fibroin, Nat. Protoc. 6 (10) (2011) 1612–1631.
- [42] Standard Test Methods for Measuring Adhesion by Tape Test, ASTM..
- [43] S.U. Siddiqui, Sapna Geeta, Mathematical modelling of blood flow through catheterized artery under the influence of body acceleration with slip velocity, Appl. Appl. Math. 8 (2) (2013) 481–494.
- [44] L. Wu, M. Huber, D. Wu, J. Chen, M. Li, Y. Ding, X. Ji, Intra-arterial cold saline infusion in stroke: historical evolution and future prospects, Aging and Disease11 (6) (2020) 1527–1536.
- [45] C. Wu, W. Zhao, H. An, L. Wu, J. Chen, M. Hussain, Y. Ding, C. Li, W. Wei, J. Duan, C. Wang, Q. Yang, D. Wu, L. Liu, X. Ji, Safety, feasibility, and potential efficacy of intraarterial selective cooling infusion for stroke patients treated with mechanical thrombectomy, J. Cerebr. Blood Flow Metabol. 38 (12) (2018) 2251–2260.
- [46] J. Chen, L. Liu, H. Zhang, X. Geng, L. Jiao, G. Li, J.M. Coutinho, Y. Ding, D. S. Liebeskind, X. Ji, Endovascular hypothermia in acute ischemic stroke: pilot study of selective intra-arterial cold saline infusion, Stroke 47 (7) (2016) 1933–1935.
- [47] A.J. Zhong, H. Kamal, A. Uddin, E. Feldstein, S.D. Shapiro, J.Y. Chung, M. Ogarro, R. Friedman, J. Simmons, G. Graifman, C. Kurian, G. Kaur, S.A. Mayer, J. Chong, C. D. Gandhi, F. Al-Mufti, Transcarotid access for mechanical thrombectomy in acute ischemic stroke: a meta-analysis and systematic review, J. Stroke Cerebrovasc. Dis. 31 (5) (2022), 106428.
- [48] E. Esposito, M. Ebner, U. Ziemann, S. Poli, In cold blood: intraarteral cold infusions for selective brain cooling in stroke, J. Cerebr. Blood Flow Metabol.: official journal of the International Society of Cerebral Blood Flow and Metabolism 34 (5) (2014) 743–752.
- [49] J. Slotboom, Localized therapeutic hypothermia in the brain for the treatment of ischemic stroke, J. appl. physiol. Bethesda, Md 102 (4) (2007) 1303–1304, 1985.
- [50] A.A. Konstas, M.A. Neimark, A.F. Laine, J. Pile-Spellman, A theoretical model of selective cooling using intracarotid cold saline infusion in the human brain, J. Appl. Physiol. (Bethesda, Md 102 (4) (2007) 1329–1340, 1985.
- [51] E.R. Johnston, Y. Miyagi, J.A. Chuah, K. Numata, M.A. Serban, The interplay between silk fibroin's structure and its adhesive properties, ACS Biomater. Sci. Eng. 4 (8) (2018) 2815–2824.
- [52] Z. Jia, M. Wen, Y. Cheng, Y. Zheng, Strategic advances in spatiotemporal control of bioinspired phenolic chemistries in materials science, Adv. Funct. Mater. 31 (2021). 2008821.
- [53] M. Golda-Cepa, K. Engvall, M. Hakkarainen, A. Kotarba, Recent progress on parylene C polymer for biomedical applications: a review, Prog. Org. Coating 140 (2020), 105493.
- [54] R.L. Hamilton, O.K. Crosser, Thermal conductivity of heterogeneous twocomponent systems, Ind. Eng. Chem. Fundam. 1 (3) (1962) 187–191.
- [55] S. Kiil, Quantitative analysis of silica aerogel-based thermal insulation coatings, Prog. Org. Coating 89 (2015) 26–34.
- [56] R. Kollmar, T. Blank, J.L. Han, D. Georgiadis, S. Schwab, Different degrees of hypothermia after experimental stroke: short- and long-term outcome, Stroke 38 (5) (2007) 1585–1589.
- [57] H.A. Choi, N. Badjatia, S.A. Mayer, Hypothermia for acute brain injury—mechanisms and practical aspects, Nature reviews, Neurology 8 (4) (2012) 214–222.
- [58] S.H. Lee, H.K. Kim, S.C. Park, E.S. Kim, T.K. Kim, C.S. Kim, The effect of infusion rate and catheter length on the temperature of warming fluid, Kor. J. Anesthesiol. 58 (1) (2010) 31–37.
- [59] S. Li, Y.L. Zhang, J.Y. Sun, Y.W. Hua, P.H. Wu, Safe temperature range for intraoperative and early postoperative continuous hyperthermic intraperitoneal perfusion in a swine model of experimental distal gastrectomy with Billroth II reconstruction, J. Transl. Med. 11 (2013) 181.